

Structural and transport properties of Bi-substituted Co_2MnO_4

Ravi Kumar,¹ S. K. Arora,^{2,a)} I. V. Shvets,² N. E. Rajeevan,³ P. P. Pradyumnan,³ and D. K. Shukla⁴

¹Materials Science Division, IUAC, New Delhi 110 067, India

²CRANN, School of Physics, Trinity College Dublin, Dublin 2, Ireland

³Department of Physics, University of Calicut, Kerala 673 635, India

⁴Department of Physics, Aligarh Muslim University, Aligarh 202 002, India

(Presented 12 November 2008; received 22 September 2008; accepted 3 November 2008; published online 12 February 2009)

We report the structural and transport properties of the Bi-substituted Co_2MnO_4 multiferroic materials. Samples synthesized using the solid state reaction route with the composition $\text{Bi}_x\text{Co}_{2-x}\text{MnO}_4$ ($0 < x < 0.3$) exhibit a single phase behavior with a cubic spinel structure (space group $Fd\bar{3}m$). The lattice parameter was found to increase with the Bi substitution. The dc-conductivity studies reveal that all the samples possess a semiconducting behavior. The resistivity was found to decrease with the increase in the Bi substitution. The dc- as well as ac-conductivity data were analyzed in the light of various conduction models. The dc-conductivity data are explained using the variable range hopping model. The ac conductivity calculated from the dielectric data as a function of temperature and frequency demonstrates the cross over from small polaron tunneling to correlated barrier hopping type conduction in these materials. © 2009 American Institute of Physics. [DOI: 10.1063/1.3067635]

I. INTRODUCTION

The coexistence of ferromagnetism/ferrimagnetism and ferroelectricity in a new class of materials termed as multiferroics (MF) has triggered an increased interest in search of new materials.^{1–7} MF materials could lead to the emergence of new storage media, which enables electrically reading/writing of the magnetic memories and vice versa, yielding more degrees of freedom from an application point of view.

Multiferroicity in conventional spinel oxides has been predicted and studied. However, the strength of magnetoelectric coupling was found to be weak.^{2,3} Chemical and physical properties of ternary spinels can be tailored by changing the cation distribution at tetrahedral and octahedral sites.^{4–8} In all spinel-like structures the oxygen parameter u has a value around 0.375 and is crucial for transport properties. For $u = 0.375$, the arrangement of O^{2-} ions are exactly a cubic close packing. A deviation from the ideal pattern occurs with $u > 0.375$, resulting in the deformation of oxygen tetrahedrons and octahedrons.^{9,10} Bismuth based magnetic pervoskites showed the ferroelectric and ferromagnetic behavior due to the covalent bonding between bismuth and oxygen atoms.¹¹

We propose to engineer a class of materials by incorporation of Bi in the spinel structure of cobalt manganite spinels (Co_2MnO_4). In our earlier work⁴ we have shown that $\text{Bi}_x\text{Co}_{2-x}\text{MnO}_4$ ($0 < x < 0.3$) exhibit a strong magnetoelectric coupling up to ~ 180 K. We present here the detailed structural and electrical properties of the $\text{Bi}_x\text{Co}_{2-x}\text{MnO}_4$ ($0.0 \leq x \leq 0.3$) system.

II. EXPERIMENTAL

The samples of $\text{Bi}_x\text{Co}_{2-x}\text{MnO}_4$ ($0.0 \leq x \leq 0.3$) were synthesized by standard solid state reaction technique. Details of

the material synthesis are given elsewhere.⁴ The crystal structure of the materials was studied at room temperature using a Bruker D8 x-ray diffractometer with $\text{Cu } K\alpha$ radiation in 2θ range of 15° – 75° . The dc-conductivity measurements were performed using the standard four-probe technique in a temperature range of 150–400 K. The temperature was controlled within ± 50 mK using a Lakeshore temperature controller. Temperature and frequency dependent dielectric measurements were performed with an HP4192 precision LCR meter. For the dielectric measurements, the surfaces of the pellets were polished and silver coated, which were kept at 200 °C for 2 h for stabilization of electrodes.

III. RESULTS AND DISCUSSION

The x-ray diffraction (XRD) patterns obtained at room temperature for $\text{Bi}_x\text{Co}_{2-x}\text{MnO}_4$, with $x = 0.0, 0.1, 0.2,$ and 0.3 , are shown in Fig. 1. The results of indexing and refinement of XRD patterns indicate the presence of a single-phase polycrystalline cubic spinel structure for the synthesized materials. All the samples correspond to the space group $Fd\bar{3}m$, as a disordered spinel in which cations occupy two non-equivalent sites: tetrahedral $8a$ (A -sites) and octahedral $16d$ (B -sites). From Fig. 1, the shift in planes toward lower 2θ with Bi substitution is clearly observed, indicating the lattice expansion due to the substitution of Co^{3+} by Bi^{3+} . The determined lattice parameters a are 8.2726, 8.3104, 8.3242, and 8.3279 Å for $x = 0, 0.01, 0.2,$ and 0.3 , respectively. The increasing trend of lattice parameter with increasing Bi content could be attributed to the fact that ionic radius of Bi^{3+} (1.17 Å) is greater than that of Co^{3+} (0.65 Å) and Mn^{3+} (0.785 Å), occupying the octahedral sites.

The dc-conductivity measured in the temperature range of 150–400 K exhibits semiconducting behavior with resistivity values between 300 and 600 Ω cm at room temperature except for sample with $x = 0$, for which it is in the order

^{a)}Electronic mail: aroras@tcd.ie.

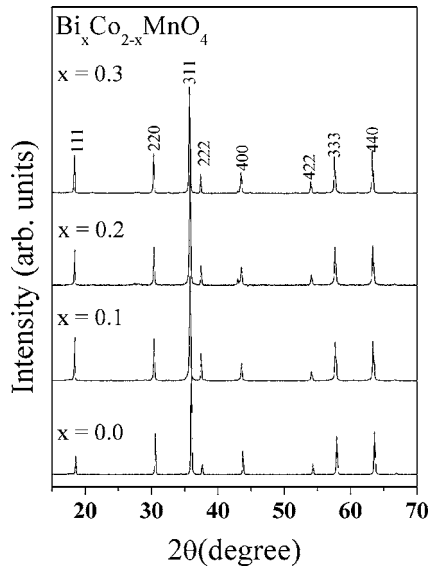


FIG. 1. XRD pattern for the $\text{Bi}_x\text{Co}_{2-x}\text{MnO}_4$ ($x=0, 0.1, 0.2,$ and 0.3) samples measured at room temperature.

of a $\text{k}\Omega\text{cm}$ (Fig. 2). Bi substitution is found to reduce the resistivity that may be due to the increase in the number of charge carriers by replacing the Co^{3+} ions in the low spin state by Bi^{3+} ions. The second most probable reason is the enhanced ionic conductivity in the presence of Bi, as reported for $\text{La}_2\text{Mo}_2\text{O}_9$ -based oxide-ion conductors.¹² The basic conduction mechanism considered is the hopping of electrons between nonequivalent octahedral and tetrahedral sites. For hopping conductivity, $\sigma_{\text{dc}}T$ is proportional to $\exp(-E_{\text{act}}/k_B T)$, as shown in Fig. 3. The activation energies (E_{act}) calculated from the plots of $\log \sigma_{\text{dc}}T$ versus $1000/T$ (Fig. 3) are 0.1813, 0.1651, 0.1628, and 0.1591 eV for $x=0, 0.1, 0.2,$ and 0.3 , respectively. The deviation from linearity in the $\sigma_{\text{dc}}T$ versus $1000/T$ plots at low temperatures, i.e., below 290 K for $x=0.0$ and below 212 K for $x=0.3$, indicates that the small polaron hopping model is valid only at relatively higher temperatures for lower Bi doping and over a wider temperature range for higher Bi doping. In the low temperature region, the conduction may follow the variable range hopping (VRH) model.^{13–15} According to VRH model, the dc conductivity σ_{dc} is proportional to $\exp(-T_0/T)^{1/4}$, with T_0

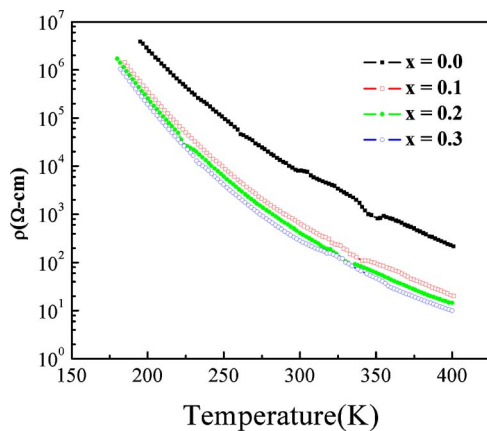


FIG. 2. (Color online) Temperature dependence of dc resistivity for $\text{Bi}_x\text{Co}_{2-x}\text{MnO}_4$ samples for $x=0, 0.1, 0.2,$ and 0.3 .

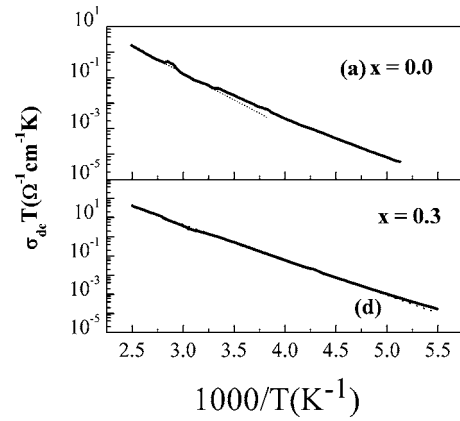


FIG. 3. $\sigma_{\text{dc}}T$ vs $1000/T$ plots for $\text{Bi}_x\text{Co}_{2-x}\text{MnO}_4$ ($x=0$ and 0.3) samples.

being the characteristic temperature. Figure 4 shows the variation in $\log \sigma_{\text{dc}}$ versus $T^{-1/4}$ which fits linearly, indicates the validity of variable range hopping mechanism. According to VRH theory,¹⁴ $k_B T_0 = 18\alpha^3/N(E)$, where $N(E)$ is the density of states and $1/\alpha$ corresponds to the localization length. From Fig. 4, we have found that the value of T_0 increased with Bi substitution ($T_0^{1/4}$ varying from $100^{1/4}$ for $x=0.0$ to $118^{1/4}$ for $x=0.3$), which points to a modification of the effective localization length.

The ac conductivity (σ_{ac}) was studied over a frequency range of 100 kHz–5 MHz, for temperature varying from 150 to 425 K. The σ_{ac} was calculated using the relation $\sigma_{\text{ac}} = \epsilon_0 \epsilon' \omega \tan \delta$. The σ_{ac} is found to be increasing in the $\text{Bi}_x\text{Co}_{2-x}\text{MnO}_4$ ($0.0 \leq x \leq 0.3$) with greater Bi content, especially in the high frequency region (see Fig. 5). This indicates that movement or hopping of the charge carrier is influenced by the neighborhood, i.e., enhanced by presence of Bi^{3+} ions with $6s^2$ lone pair electrons. At higher frequencies (~ 2 MHz), σ_{ac} is decreased for all compositions (not shown here), indicating the inability of hopping of charges to follow the high frequency of the applied field. For semiconductors and disordered systems, the ac conductivity follow the power law behavior with frequency expressed as¹⁶ $\sigma_{\text{ac}}(\omega) = A\omega^s$, where A is temperature dependent constant and s is the frequency exponent ($s \leq 1$). From the log-log plots drawn for

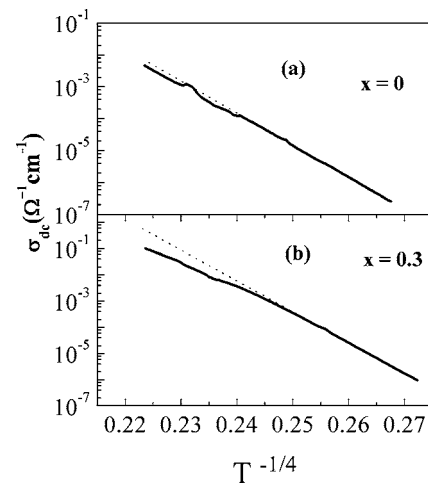


FIG. 4. σ_{dc} vs $T^{-1/4}$ plots for $\text{Bi}_x\text{Co}_{2-x}\text{MnO}_4$ ($x=0$ and 0.3).

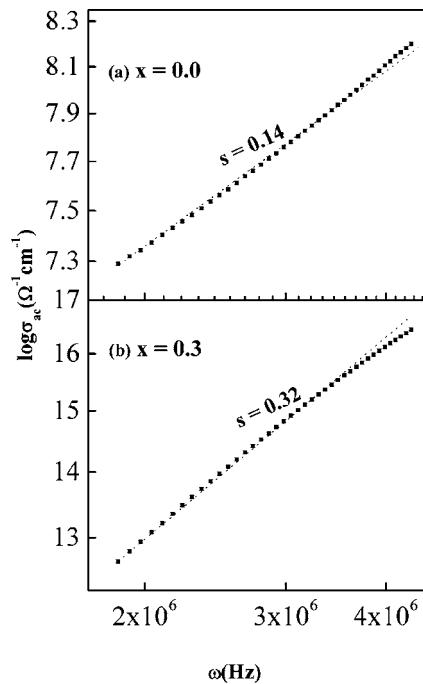


FIG. 5. $\log \sigma_{ac}$ vs $\log \omega$ at 300 K for $\text{Bi}_x\text{Co}_{2-x}\text{MnO}_4$ ($x=0$ and 0.3).

σ_{ac} versus ω (see Fig. 5, $\log \sigma_{ac}$ versus $\log \omega$ at room temperature) for the different compositions, the slope directly provides the value of dimensionless frequency exponent s and it is clear that frequency exponent s varies with Bi content.

The temperature dependence of frequency exponent s is shown in Fig. 6. Initially the temperature dependence of s increases and then decreases and finally shows almost temperature independent behavior at higher temperatures. The frequency exponent s is a measure of correlation between σ_{ac} and frequency. For random hopping of carriers, s should be 0 (frequency independent σ_{ac}) and tends to approach 1 as correlation increases. Qualitatively small polaron (SP) tunneling

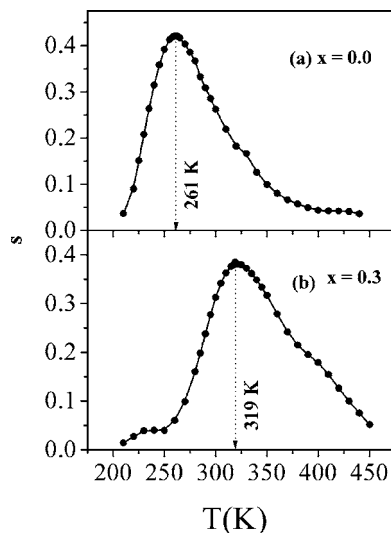


FIG. 6. Temperature dependence of frequency exponent s for $\text{Bi}_x\text{Co}_{2-x}\text{MnO}_4$ ($x=0$ and 0.3).

is usually associated with an increase in s with increasing temperature, indicating the activated behavior of polarons, which is independent of intersite separation. On the other hand, correlated barrier hopping (CBH) shows a decrease in s with increasing temperature, which indicates the thermally activated behavior of electron transfer over the barrier between two sites having their own Coulombic potential wells. Temperature dependence arising from the correlation between barrier height and intersite separation is the characteristics of CBH model.¹⁶ From Fig. 6 it is clear that for pure Co_2MnO_4 , the frequency exponent s is found to increase up to 260 K and then decrease. For this sample, SP model is suitable up to 260 K at which maximum correlation is exhibited between σ_{ac} and frequency. Above 260 K, CBH model is valid, where dc-conductivity contribution is not negligible. For the Bi-substituted samples also, SP and CBH models together seem to cover the total measured temperature range. However, in the case of Bi-substituted samples the temperature limit for SP model is extended to a higher temperature (up to ~ 320 K) than that of the pure one.

IV. CONCLUSIONS

In conclusion, single-phase polycrystalline samples of $\text{Bi}_x\text{Co}_{2-x}\text{MnO}_4$ ($0.0 \leq x \leq 0.3$) have been prepared using a conventional solid state reaction. Analysis of XRD data shows that Bi content above $x=0.3$ is difficult to accommodate, while retaining the cubic spinel structure. The dc-conductivity analysis revealed the semiconducting nature of these compounds and conductivity increases with Bi substitution. The value of frequency exponent s estimated from ac-conductivity measurements over wide range of temperature is found to follow two models, namely, the SP tunneling model and the CBH model from lower (SP up to ~ 260 K for pure and up to ~ 320 for Bi substituted) to higher temperature side, respectively.

¹W. Eerenstein, N. D. Mathur, and J. F. Scott, *Nature (London)* **442**, 759 (2006).

²J. F. Scott, *Rep. Prog. Phys.* **42**, 1055 (1979).

³M. Fiebig, *J. Phys. D* **38**, R123 (2005).

⁴N. E. Rajeevan *et al.*, *Appl. Phys. Lett.* **92**, 102910 (2008).

⁵S. Kondo, D. C. Johnston, C. A. Swenson, F. Borsa, T. Gu, A. I. Goldman, M. B. Maple, D. A. Gajewski, E. J. Freeman, N. R. Dilley, R. P. Dickey, J. Merrin, K. Kojima, G. M. Luke, Y. J. Uemura, O. Chmaissem, and J. D. Jorgensen, *Phys. Rev. Lett.* **78**, 3729 (1977).

⁶N. Fujiwara, H. Yasuoka, and Y. Ueda, *Phys. Rev. B* **57**, 3539 (1998).

⁷J. L. Dormann and M. Nogués, *J. Phys.: Condens. Matter* **2**, 1223 (1990).

⁸G. Srinivasan, E. T. Rasmussen, and R. Hayes, *Phys. Rev. B* **67**, 014418 (2003).

⁹E. J. W. Verwey and E. L. Heilmann, *J. Chem. Phys.* **15**, 174 (1947).

¹⁰Y. Ikedo, J. Sugiyama, H. Nozaki, H. Itahara, J. H. Brewer, E. J. Ansaldo, G. D. Morris, D. Andreica, and A. Amato, *Phys. Rev. B* **75**, 054424 (2007).

¹¹W. Prellier, M. P. Singh, and P. Murugavel, *J. Phys.: Condens. Matter* **17**, R803 (2005).

¹²Q. F. Fang, F. J. Liang, X. P. Wang, G. G. Zhang, and Z. J. Cheng, *Mater. Sci. Eng., A* **442**, 43 (2006).

¹³V. Massarotti, D. Capsoni, M. Bini, and G. Chiodelli, *J. Solid State Chem.* **131**, 94 (1997).

¹⁴N. F. Mott, *J. Non-Cryst. Solids* **1**, 1 (1968).

¹⁵M. Viret, L. Ranno, and J. M. D. Coey, *Phys. Rev. B* **55**, 8067 (1997).

¹⁶S. R. Elliott, *Adv. Phys.* **36**, 135 (1987).